 doi:10.1111/jfd.12444

Morphological diversity of *Paramoeba perurans* trophozoites and their interaction with Atlantic salmon, *Salmo salar* L., gills

J Wiik-Nielsen[1], T A Mo[1], H Kolstad[2], S N Mohammad[1], S Hytterød[1] and M D Powell[3]

1 Norwegian Veterinary Institute, Oslo, Norway
2 Imaging Centre, Norwegian University of Life Sciences, Ås, Norway
3 Norwegian Institute for Water Research, Bergen, Norway

Abstract

Amoebic gill disease (AGD) caused by the ectoparasite *Paramoeba perurans* affects several cultured marine fish species worldwide. In this study, the morphology and ultrastructure of *P. perurans in vitro* and *in vivo* was investigated using scanning and transmission electron microscopy (SEM and TEM, respectively). Amoebae cultures contained several different morphologies ranging from a distinct rounded cell structure and polymorphic cells with pseudopodia of different lengths and shapes. SEM studies of the gills of AGD-affected Atlantic salmon, *Salmo salar* L., revealed the presence of enlarged swellings in affected gill filaments and fusion of adjacent lamellae. Spherical amoebae appeared to embed within the epithelium, and subsequently leave hemispherical indentations with visible fenestrations in the basolateral surface following their departure. These fenestrated structures corresponded to the presence of pseudopodia which could be seen by TEM to penetrate into the epithelium. The membrane–membrane interface contained an amorphous and slightly fibrous matrix. This suggests the existence of cellular glycocalyces and a role for extracellular products in mediating pathological changes in amoebic gill disease.

Correspondence *J Wiik-Nielsen, Norwegian Veterinary Institute, PO Box 750 Sentrum, 0106 Oslo, Norway (e-mail: jannicke.wiik@vetinst.no)*

Keywords: amoebic gill disease, gill epithelium, glycocalyx, pseudopodia, scanning electron microscopy.

Introduction

Amoebic gill disease (AGD) caused by the amphizoic amoeba *Paramoeba perurans* (syn. *Neoparamoeba perurans*, see Feehan *et al.* 2013) has recently become a disease of significance to Atlantic salmon, *Salmo salar* L. and rainbow trout, *Oncorhynchus mykiss* (Walbaum) aquaculture in Northern Europe. AGD has been reported from farmed salmonids in a number of countries including Australia, USA, Ireland, Spain, New Zealand, France, Scotland, Norway, Chile and South Africa (Kent, Sawyer & Hedrick 1988; Munday *et al.* 1993; Rodger & Mcardle 1996; Nowak *et al.* 2002; Steinum *et al.* 2008; Bustos *et al.* 2011; Mitchell & Rodger 2011; Mouton *et al.* 2014). In addition, *P. perurans* is also believed to be responsible for gill disease in turbot, *Scophthalmus maximus* (L.), European seabass, *Dicentrarchus labrax* (L.), sharp snout sea bream, *Diplodus puntazzo* (Walbaum), ayu, *Plecoglossus altivelis* (Temminck & Schlegel), blue warehou, *Seriolella brama* Günther, olive flounder, *Paralichthys olivaceus* (Temminck & Schlegel) and recently in ballan wrasse, *Labrus bergylta* Ascanius (Dyková & Novoa 2001; Dyková *et al.* 2005; Kim *et al.* 2005; Adams, Villavedra & Nowak 2008; Crosbie *et al.* 2010; Santos *et al.* 2010; Karlsbakk *et al.* 2013). Identified as the

Journal of Fish Diseases

cosmopolitan agent of AGD (Young *et al.* 2008), *P. perurans* has been cultured *in vitro* and fulfils Koch's postulates in challenge studies (Crosbie *et al.* 2012). In Norway, since its first association with gill disease and diagnosis as a sole agent of disease (Steinum *et al.* 2008), outbreaks have increased and spread northward with 69 cases being diagnosed in 2014 by the Norwegian Veterinary Institute (Bornø & Linaker 2015).

AGD-associated pathological changes involve acute branchial epithelial hyperplasia and the formation of characteristic hyperplastic plaques on the gills (Roubal, Lester & Foster 1989; Munday *et al.* 1993). Several studies have investigated *P. perurans* and its association to the gills at the ultrastructural level. Kent *et al.* (1988) showed ultrastructural characteristics of *Neoparamoeba pemaquidensis* (initially considered to be the aetiological agent of AGD and possible represented *P. perurans*) including a pronounced cellular glycocalyx around the amoeba trophozoite and the presence of an endosymbiotic parasome, a *Perkinsela amoebae*-like organism (Dyková, Fiala & Peckova 2008; Young *et al.* 2014) which is a pronounced characteristic for the genera *Neoparamoeba* and *Paramoeba*. The ultrastructural morphology of cultured *Paramoeba* sp. has been described (Dyková, Figueras & Peric 2000; Dyková *et al.* 2005; Kim *et al.* 2005), and the interaction between *Paramoeba* sp. and hyperplastic gill lesions in AGD-affected Atlantic salmon has been examined (Roubal *et al.* 1989; Lovy *et al.* 2007) with primary focus on the response of gill hyperplastic tissues to infection and presence of the amoebae including description of a novel type of eosinophils and the presence of dendritic-like cells.

Although histologically *P. perurans* commonly is identified in close apposition to the branchial epithelium, the intimate nature of this association is not clear and the amoeba–gill epithelial cell interaction requires further examination. In the present study, the morphologies of cultured *P. perurans* and the surface relationships between *P. perurans* and the Atlantic salmon gill epithelium affected by AGD are described using scanning and transmission electron microscopy (SEM and TEM, respectively).

Materials and methods

Paramoeba perurans culture

P. perurans were isolated from the gills of AGD-affected Atlantic salmon according to Morrison, Crosbie & Nowak (2004). From this isolate, a single trophozoite of *P. perurans* was inoculated on malt yeast agar with filtered seawater overlay (34 ppt) and cultured *in vitro* to establish a monoclonal culture according to (Crosbie *et al.* 2012). The amoebae were cultured at 15 °C and subcultured every second week. The cultures were frequently tested by qPCR to verify the presence of *P. perurans* using the method described by Fringuelli *et al.* (2012). After approximately 8 weeks, amoebae were carefully collected from the agar surface and the seawater overlay and centrifuged at 12 000***g*** for 1 min to concentrate the amoebae. Most of the supernatant was removed and the remaining concentrated suspension of amoebae was fixed with 1.25% glutaraldehyde and 2% paraformaldehyde in 0.1 M sodium cacodylate buffer (SCB) and further processed for electron microscopy to examine different amoebic morphologies seen in culture.

Infection challenge and gill sampling

Gill sampling for the present study was performed as part of a larger study relating to pathogenesis of AGD. The infection challenge was performed at Solbergstrand Research station, Norwegian Institute for Water Research, Drøbak. Atlantic salmon post-smolts, age 1 + ($N = 120$) of mean mass (±SEM) 278.0 g (±9.2 g) and fork length 28.8 cm (±0.3 cm), grown at Solbergstrand Research station, were distributed equally between 3 × 800-L square fibreglass tanks. The experimental set-up was design as a flow through system. The fish was acclimated to the test conditions for 2 weeks prior to the experiment. The experimental tanks were supplied with flowing filtered sea water (34 ppt) at 15 ± 1 °C under 12L:12D lighting conditions. Fish were fed *ad libitum* to satiation daily on a commercial pelleted diet (Skretting, Norway). Gills were screened prior to experimentation by histology to verify that fish were free from pathological changes and screened using the qPCR method mentioned above to verify the absence of *P. perurans*. The water flow to the tanks was stopped and cultured amoebae were added to two of the tanks to generate a challenge concentration of 2000 amoebae L^{-1} for 1 h. The remaining tank was not inoculated with amoebae, serving as a control.

Fourteen days post-infection, inspection of the gills showed the presence of white raised patches

on all hemibranchs equivalent to a semi-quantitative visual gill score 3–4 (Taylor *et al.* 2009) and histological examination showed typical AGD pathological changes consisting of epithelial hyperplasia in association with amoebae. A total of 10 infected fish (5 fish from each of the infected tanks) and 10 control fish were collected for ultrastructural examination of the gills. Fish were removed by dip-netting and killed with an overdose of tricaine methanesulphonate (100 mg L^{-1}) (Sigma-Aldrich, Oslo, Norway) for approximately 10 min. To reduce blood influence under the SEM investigation, the fish were bled from the caudal vessels. Then, the second gill arch on the right side was carefully dissected. Some filaments from the apex of the gill arch were stored in RNA*Later*™ for subsequent qPCR verification of the presence of *P. perurans* using the method described previously. The remaining part of the gill arch was fixed in 1.25% glutaraldehyde and 2% paraformaldehyde in 0.1 M SCB for electron microscopic examination.

Scanning electron microscopy

The fixed amoebae culture and gill arches for SEM examination were washed thoroughly in 0.1 M SCB and dehydrated with 10 min steps in ascending ethanol series (50–100%). The samples were processed in a BAL-TEC Critical Point Dryer (CPD 030, Germany), and a thin conductive coating of gold/palladium was applied to the samples using a Polaron Sputter Coater (SC 7640, UK). The coated samples were mounted on brass stubs, examined and photographed with a Zeiss EVO-50-EP scanning electron microscope at an accelerating voltage of 20 kV in the secondary emission mode.

Transmission electron microscopy

The fixed amoeba culture for ultrastructural study was washed with 0.1 M SCB and embedded in 3% low-melting agarose. Both the embedded amoebae culture and gill arches were post-fixed in 1% osmium tetroxide in 0.1 M SCB for 2 h, washed and dehydrated as described above. The amoebae culture and the tissues were embedded in LR White resin (London Resin Company, EMS, England). Semi-thin sections (1 μm) were cut from each piece of gill tissue, stained with toluidine blue and examined by light microscopy to select areas where amoebae and gill surface were observed. Ultrathin sections (60 nm) of these areas were obtained with a Leica EM UC6 Ultramicrotome. The sections were stained with 4% uranyl acetate and 1% potassium permanganate for 10 min and examined and photographed with a FEI Morgagni 268 transmission electron microscope operated at 80 kV.

Results

Morphology and ultrastructure of cultured *P. perurans*

Monoclonal cultured *P. perurans* formed both polymorphic amoeboid morphologies and distinctly rounded morphologies as seen by phase contrast microscopy (Fig. 1a). Under scanning electron microscopy, a distinctive series of morphologies could be seen. These included amoebae displaying rounded cell morphology (Fig. 1b), with short and intermediate length pseudopodia (Fig. 1c,d) and with long thin, elongate pseudopods (Fig. 1e). The intermediate morphology was most commonly observed. Ultrastructurally, the cultured amoebae were surrounded by bacteria and had a clearly defined plasma membrane and numerous endocytotic vesicles (Fig. 1f).

Morphology of gills infected by *P. perurans*

All of the fish sampled from the infected tanks were positive by qPCR for *P. perurans* and had a gross gill score of 3–4 based on the Taylor *et al.* (2009) scoring system. Similarly, none of the control fish were positive by qPCR for *P. perurans*. Under scanning electron microscopy, the gills of control fish showed a typical teleost morphology with several filaments extending from the arch forming a hemibranch (Fig. 2a) with lamellae extending perpendicularly from the filament (Fig. 2c). The gills from AGD-affected fish showed similar morphologies but with some noticeably swollen filaments (Fig. 2b) and fusion of adjacent lamellae (Fig. 2d). Notably, the remaining lamellae appeared unaffected displaying similar morphology to that of lamellae in control gills. Unaffected (control) gills displayed a flattened lamellar surface with the pavement cells having a fine microridged surface and distinctive perimeter (Fig. 2e). On AGD-affected lamellae,

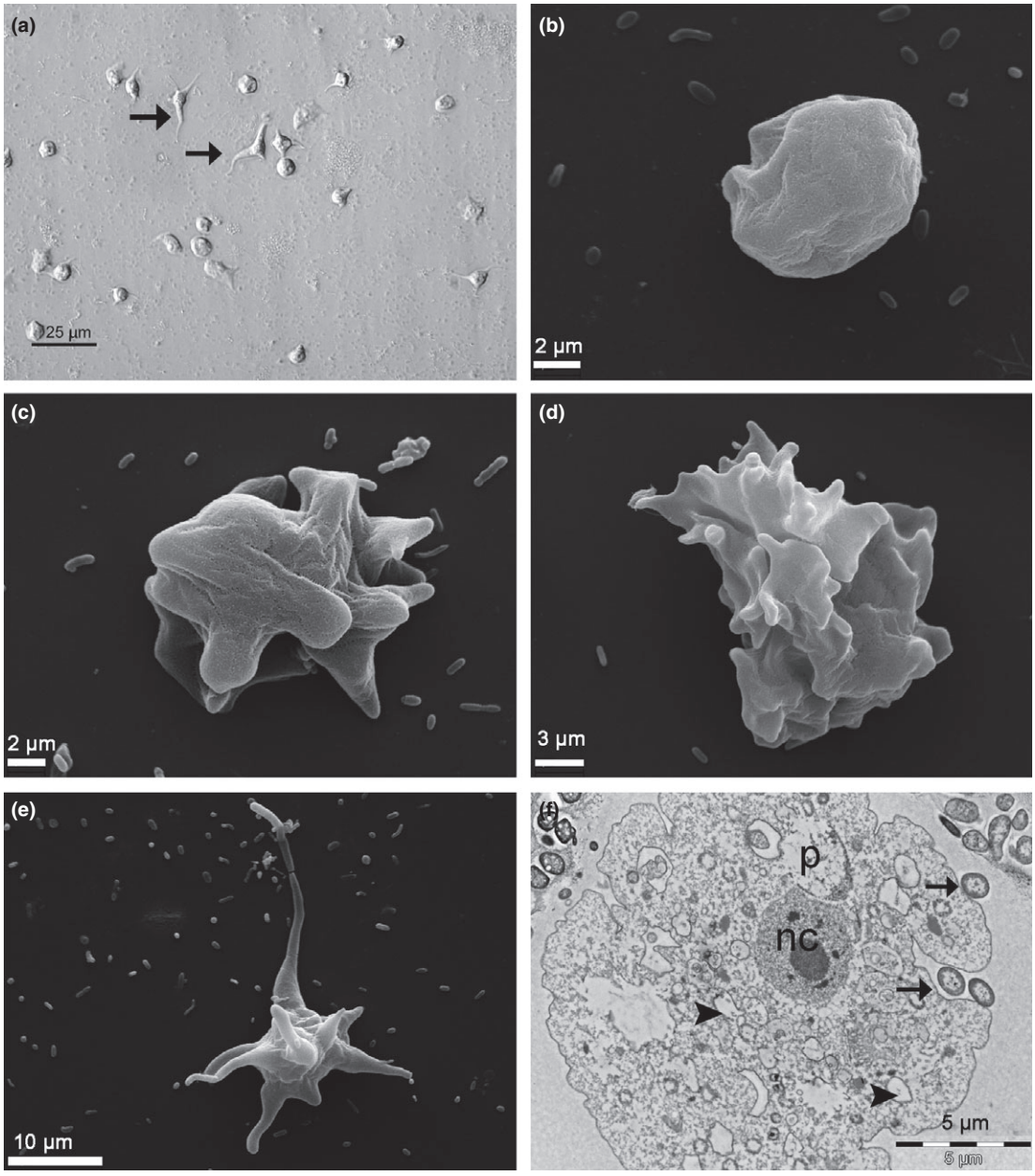

Figure 1 Microscopy of cultured *Paramoeba perurans*. (a) Phase contrast microscopy showing several morphologies of monocultured amoebae with prominent pseudopodia (arrow). (b–e) Scanning electron microscopy of the Paramoebae showing a distinctive series of morphologies including (b) rounded cell morphology, (c) short, (d) intermediate and (e) long pseudopodia. (f) Transmission electron microscopy of the amoeba in culture surrounded by bacteria (arrow). The plasma membrane is clearly defined and contains numerous endocytotic vesicles (arrowhead) and the nucleus (nc) and parasome is shown (p).

the microridge structure on the pavement cells was irregular and indistinct. Additionally, lamellae often were fused with a surface frequently populated by amoebae and prominent exfoliating cells (Fig. 2f).

P. perurans attachment to and penetration of the gill epithelium

In the interstitial region between gill hemibranchs, amoebae extensively colonized the affected area.

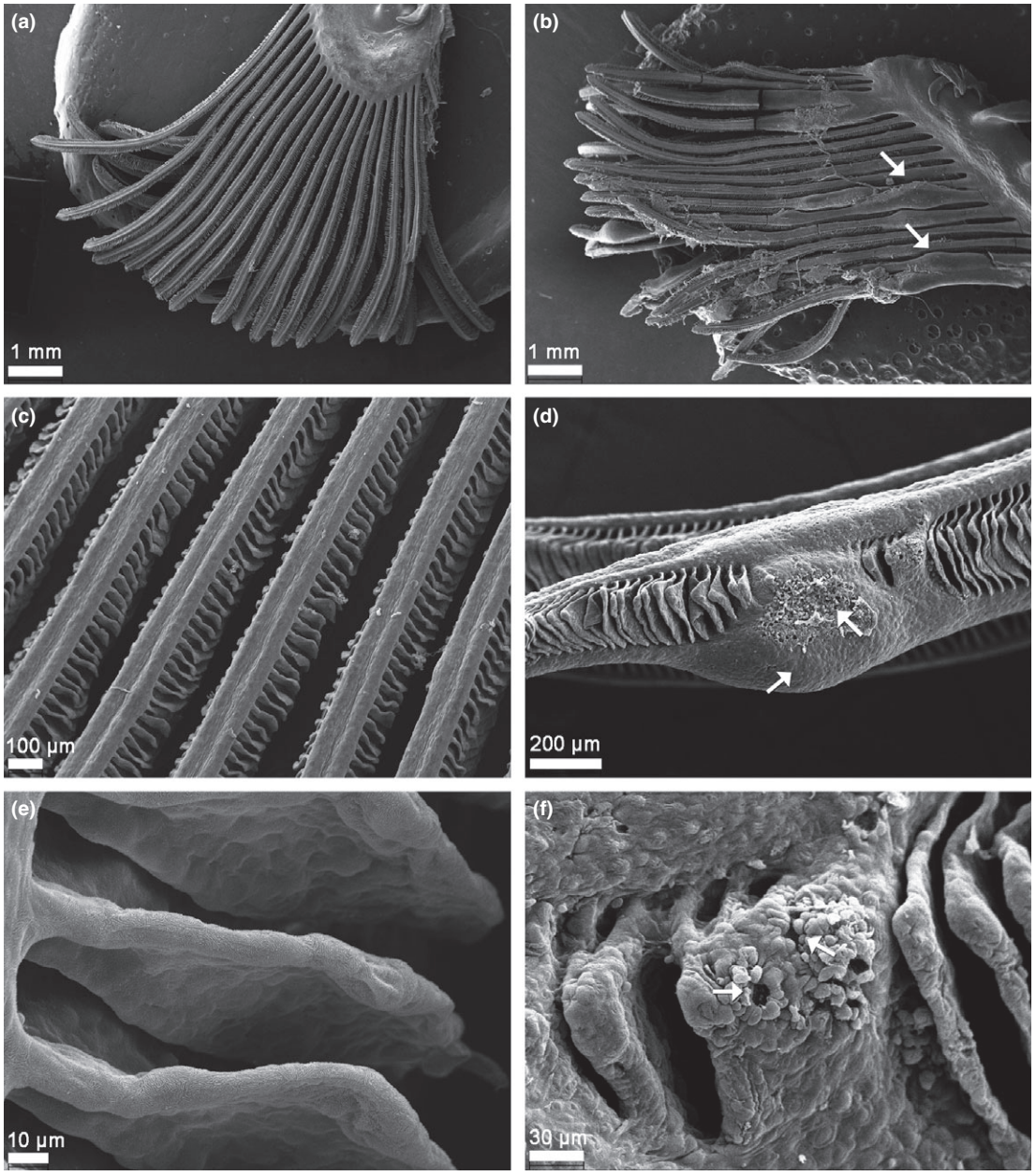

Figure 2 Scanning electron micrographs of gill filaments from healthy Atlantic salmon (images on the left A, C and E) and gill filaments infected by *Paramoeba perurans* on the right (b, d and f). Healthy gill filaments are characterized by perpendicular lamellae (c) covered by a microridged pavement epithelium (e). Infected gills show hyperplastic filamental lesions with associated amoebae appears as a swelling on the filament (b and d, arrow), the surface of which is associated with colonies of amoebae and exfoliating cells (f). Syncytia of adjacent lamellae with amoebae and exfoliating cells associated with the adjoining tissue (arrow).

This colonization was often extensive with a mix of amoebae and exfoliating cells (Fig. 3a,b). The amoebae were seen in close apposition with the pavement epithelial surface creating what appeared to be indentations in the epithelial surface (Fig. 3c–e). Following departure of the amoebae, pronounced fenestrations were visible in the indentation (Fig. 3f). The microridge structure on cells immediately apposed to the amoebae and the indentation was degenerated and the continuous flowing microridge whorls were altered. The periphery of affected pavement cells appeared to

swell and extrude towards the apical surface of adjacent cells (Fig. 3d–f). Ultrastructural study showed penetration of amoebae pseudopodia into affected pavement cells and no epithelial microridges were evident (Figs. 3g,h and 4a–d). Amoebae were often seen with a clearly visible nucleus and intracellular inclusions consistent with phagosomes and endosomes. The characteristic parasome was only occasionally observed, and when apparent, it was pale and hardly visible (Fig. 3g).

Membrane–membrane interaction between *P. perurans* and gill epithelial cells

Amoebae infiltrating the epithelial cells (Fig. 4a,c) showed an amorphous matrix surrounding the pseudopodia between the amoebic plasma membrane and the epithelial cell (Fig. 4b,d). In most instances, amoebae were observed without direct contact with the epithelial membrane, but the shape of the amoebae appeared to conform to the shape of the epithelial cell membranes (Fig. 4d). When apparent membrane–membrane interaction between amoebae and epithelial cells could be observed, no cell–cell junctions were evident (Fig. 4b). At the juncture of the pseudopodium and pavement epithelial cells, electron-dense deposits were seen below the epithelial membrane (Figs. 3h and 4c,d).

Discussion

Most studies of *Paramoeba* and *Neoparamoeba* spp. have focused on cell morphology based upon light microscopic observations (e.g. see reviews by Mitchell & Rodger (2011); Munday *et al.* (1993); Powell *et al.* (2008); Rodger & Mcardle (1996)) accompanied by transmission electron microscopy of the cultured amoebae (Kent *et al.* 1988; Roubal *et al.* 1989; Dyková *et al.* 2000, 2005; Kim *et al.* 2005; Lovy *et al.* 2007). In the present study, different morphologies of *P. perurans* were observed using scanning electron microscopy. Often large numbers of rounded amoebae were observed in dense cultures and when subculturing was infrequently performed. It has been speculated if this stage may be characteristic of a response to either limited surface area for attachment, nutrients, or in response to other environmental stressors. Similarly, the frequently observed floating stages with extended pseudopodia is presumed to have the function to maintain the amoeba in suspension (Page 1983; Van Haastert 2011) and may be involved in transmission of the amoeba in the marine environment. Ultrastructurally, the cultured amoebae shared the same morphological characteristics and an endosymbiont, as described for all species of the genera *Paramoeba* and *Neoparamoeba* (Kent *et al.* 1988; Dyková *et al.* 2000, 2005, 2007; Lovy *et al.* 2007). In the AGD tissue samples, the parasome was usually not visible, probably due to damage during the handling prior to fixation and/or the tissue processing for TEM.

In vivo evidence suggests that hyperplastic lesions are initiated by the initial individual association of trophozoites with the lamellar epithelium (Zilberg & Munday 2000; Adams & Nowak 2004; Morrison *et al.* 2004). The fusion of adjacent gill lamellae is commonly described in a number of gill diseases including AGD (e.g. Adams & Nowak 2003) and bacterial gill disease, BGD (Speare *et al.* 1991a,b). In AGD, lamellar fusion occurs typically in the early development of lesions. Adams & Nowak (2003) indicated that branchial hyperplasia begins in the interstitial tissue between lamellae followed by progressive fusion of lamellae. This is consistent with colonization of the hyperplastic lesions observed by SEM in our study, including the colonization of tissues surrounding the periphery of hyperplastic lesions where epithelial squamation may have occurred. It also seems that the amoebae colonized the interstitial region between the hemibranchs where water flow is likely to be the lowest.

Figure 3 (a) Paramoebae colonization and exfoliating cells in the interstitial region between gill hemibranchs where water flow is likely to be the lowest (arrow). (b) Close-up of the colonization of the filamental epithelium between adjacent lamellae with amoebae (arrow) and exfoliating cells (ex). (c–e) Scanning electron micrographs of *Paramoeba perurans* (a) in close association with the pavement epithelial cells (ec) and surrounded by exfoliating cells (ex) and cellular debris. (f) *P. perurans* associated indentations (i) and holes (arrow) in the plasma membrane from penetrating pseudopodia. This is supported by transmission electron micrographs (g and h) where *P. perurans* with pseudopodia (ps) is penetrating epithelial cells creating the fenestrations. (g) Bacteria are observed (arrow) and what appears to be a parasome (*) is seen in close association with the nucleus (nc). (h) At the juncture of the pseudopodium and pavement epithelial cell, electron-dense deposits are seen below the epithelial membrane (arrowhead).

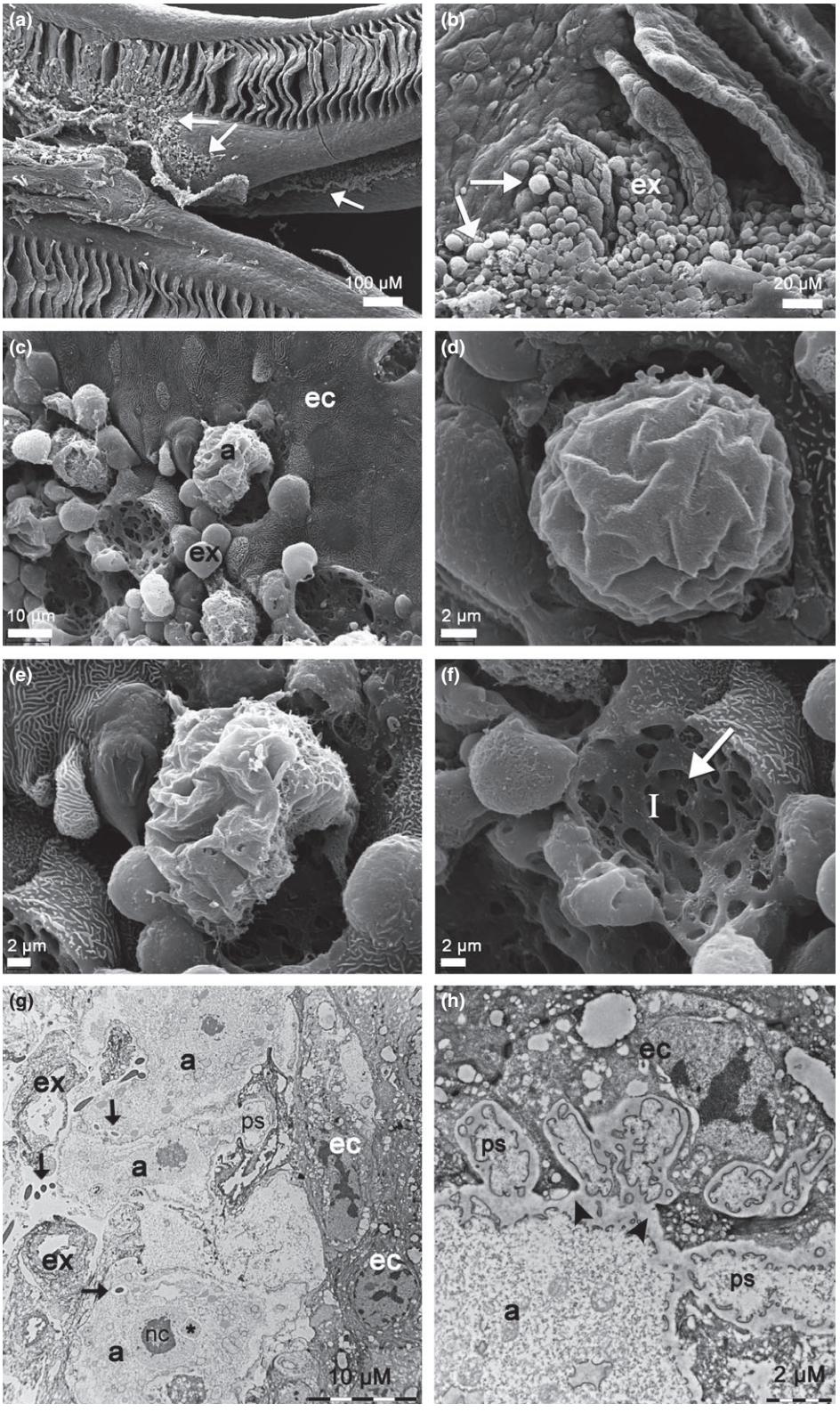

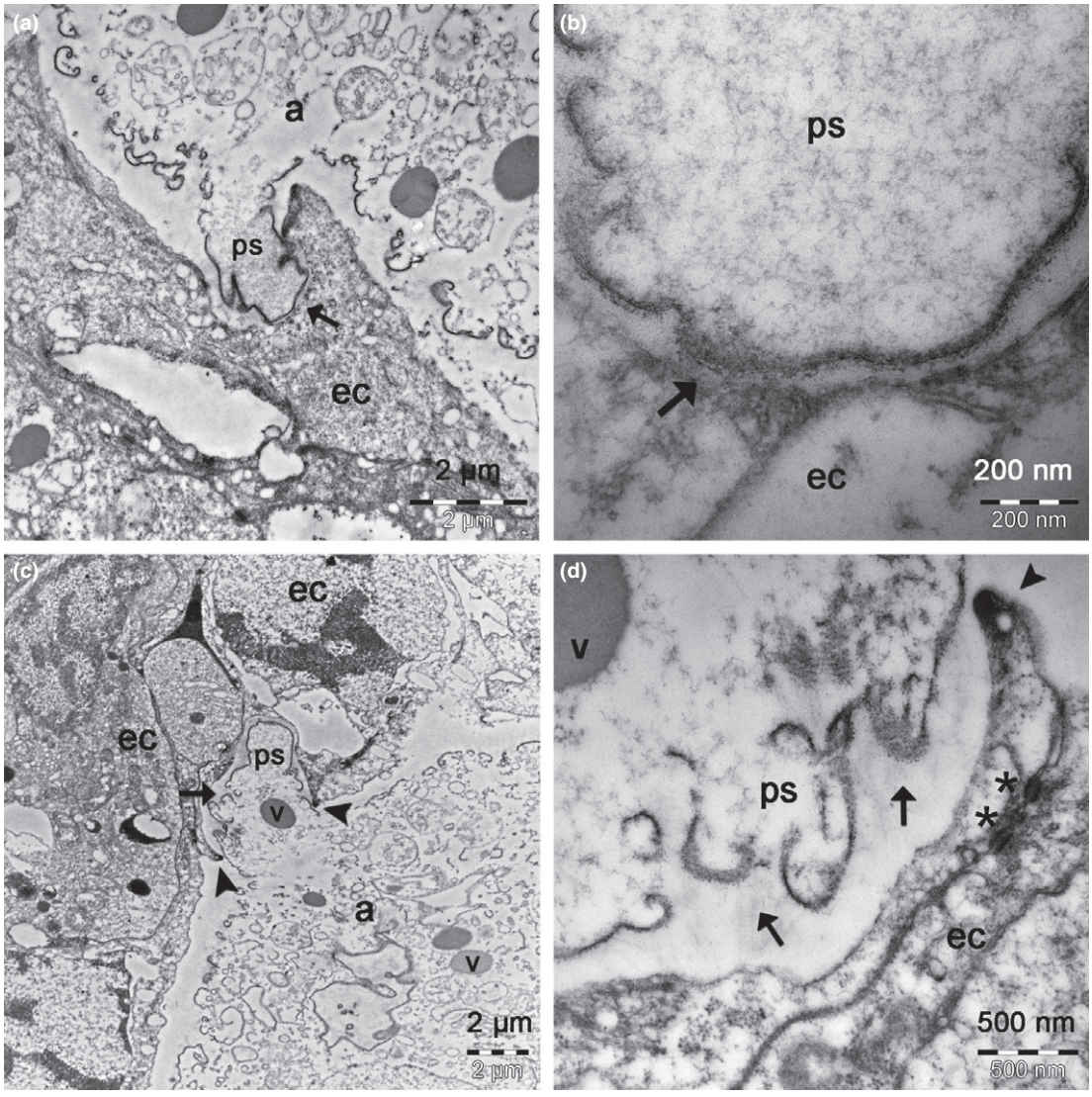

Figure 4 Transmission electron micrographs of *Paramoeba perurans* in close association with the gill epithelium. Infiltration of amoebae to the epithelial cell (a and c) with amoebic and epithelial plasma membranes in close apposition (b) (arrow) and marked interstitial amorphous matrix (d) (arrow) with associated electron densities of the amoebic plasma membrane and pavement epithelial cell (arrowhead). * indicates pavement epithelial cell tight junctions.

Colonization of the epithelial surface was associated with amoebae, cellular debris and rounded exfoliating cells that seemed to be sloughed away from the underlying tissue. This observation was supported by ultrastructural examination and is consistent with previous studies (Zilberg & Munday 2000; Lovy *et al.* 2007).

Association of *P. perurans* with the pavement epithelial cell membranes showed that amoebae appear to nestle within the epithelium. The amoebae displayed a rounded, rather wrinkled morphology at the gill surface. This is probably due to the handling before fixation (e.g. anaesthetic) and/or the tissue processing for SEM (e.g. shrinkage artefact). Most frequently, the indentations were observed without the amoebae attached. It might be that the amoebae have 'moved on' from the dead epithelial cell and the fenestrated indentation remains. More likely, the amoebae may have been lost as a result of handling or processing as mentioned above. The mucous coat on the gill lamellae was seldom

visible, probably being washed away or dissolved more quickly than it was stabilized (Lumsden *et al.* 1994; Allan-Wojtas *et al.* 1997). The loss of the mucous layer exposed the epithelial surface and made it possible to study the amoebae interaction and influence on the gill epithelial cells, but it also may have made the amoebae more vulnerable throughout the processing.

Ultrastructural evidence suggests that pseudopodia were extruded into the affected epithelial cell resulting in the obvious fenestration of the epithelium. This is consistent with previous studies (Roubal *et al.* 1989; Lovy *et al.* 2007). Amoebae were usually observed without direct contact with the epithelial membrane, but conform shape of the membranes suggests that the original contact has been close. The space between the membranes is probably a shrinkage artefact caused by the fixation and/or processing of the tissue samples (Roubal *et al.* 1989; Lovy *et al.* 2007). The membrane–membrane interface contained an amorphous and slightly fibrous matrix. This suggests the existence of cellular glycocalyx, but can also be a result of contraction of the amoebae away from the epithelial cells during the tissue handling as mentioned above (Roubal *et al.* 1989). Amoebic attachment to the gill has been a focus for many studies (Butler & Nowak 2004; Lee *et al.* 2006; Bridle *et al.* 2015). High-molecular-weight antigenic (HMWA) glycoproteins that appear to be anchored into the amoeba plasma membrane, identified by immunogold labelling are present within an apparent cell membrane glycocalyx (Villavedra *et al.* 2010). Evidence suggests that *Neoparamoeba* sp. may produce cytotoxic extracellular products *in vitro* (Butler & Nowak 2004; Lee *et al.* 2006; Bridle *et al.* 2015) in salmon gill epithelial cell cultures. These data correspond with the current observations that tight membrane–membrane interaction is not necessary for induction of pavement cell epithelial necrosis by *P. perurans*. It is well established that other free-living or amphizoic amoeba species, for example *Acanthamoeba* spp., and obligate parasitic species such as *Entamoeba* spp. produce extracellular products capable of inducing cytopathic effects (Serrano-Luna *et al.* 2013). However, the mechanism by which they are induced, produced and secreted by *Paramoeba* spp. is not known.

In conclusion, *P. perurans* under culture conditions presented a number of different morphologies including rounded cells and extended pseudopodia characteristic of amoebae. When used in an acute challenge of Atlantic salmon, *P. perurans* appeared to attach to the gill surface and attack individual epithelial cells. The amoeba–epithelial cell interaction resulted in fenestrated indentations of the gill epithelium of pavement epithelial cells. The amoeba–epithelial cell interaction typically consisted of close but not direct membrane–membrane attachment, possible representing interaction of cellular glycocalyces.

Acknowledgement

The authors would like to thank Duncan Colquhoun and Trude Vrålstad for helpful comments on the manuscript. We will also thank Joachim Johansen at the NIVA Solbergstrand Marine Research Station for assistance in fish maintenance and sampling and the Norwegian research council (project number 233858/E40) for financial support.

References

Adams M.B. & Nowak B.F. (2003) Amoebic gill disease: sequential pathology in cultured Atlantic salmon, *Salmo salar* L. *Journal of Fish Diseases* **26**, 601–614.

Adams M.B. & Nowak B.F. (2004) Experimental amoebic gill disease of Atlantic salmon, *Salmo salar* L.: further evidence for the primary pathogenic role of *Neoparamoeba* sp. (Page, 1987). *Journal of Fish Diseases* **27**, 105–113.

Adams M.B., Villavedra M. & Nowak B.F. (2008) An opportunistic detection of amoebic gill disease in blue warehou, *Seriolella brama* Günther, collected from an Atlantic salmon, *Salmo salar* L., production cage in south eastern Tasmania. *Journal of Fish Diseases* **31**, 713–717.

Allan-Wojtas P., Farnworth E.R., Modler H.W. & Carbyn S. (1997) A solvent-based fixative for electron microscopy to improve retention and visualization of the intestinal mucus blancet for probiotic studies. *Microscopy Research and Technique* **36**, 390–399.

G. Bornø & M.L. Linaker (eds) (2015) Fish Health Report 2014. Norwegian Veterinary Institute, ISSN 1893-1480 electronic edition.

Bridle A.R., Davenport D.L., Crosbie P.B.B., Polinski M. & Nowak B. (2015) *Neoparamoeba perurans* loses virulence during clonal culture. *International Journal for Parasitology* **45**, 575–578.

Bustos P.A., Young N.D., Rozas M.A., Bohle H.M., Ildefonso R.S., Morrison R.N. & Nowak B.F. (2011) Amoebic gill disease (AGD) in Atlantic salmon (*Salmo salar*) farmed in Chile. *Aquaculture* **310**, 281–288.

Butler R. & Nowak B.F. (2004) In vitro interactions between *Neoparamoeba* sp. and Atlantic salmon epithelial cells. *Journal of Fish Diseases* **27**, 343–349.

Crosbie P.B., Ogawa K., Nakano D. & Nowak B.F. (2010) Amoebic gill disease in hatchery-reared ayu, *Plecoglossus altivelis* (Temminck & Schlegel), in Japan is caused by *Neoparamoeba perurans*. *Journal of Fish Diseases* **33**, 455–458.

Crosbie P.B., Bridle A.R., Cadoret K. & Nowak B.F. (2012) In vitro cultured *Neoparamoeba perurans* causes amoebic gill disease in Atlantic salmon and fulfils Koch's postulates. *International Journal of Parasitology* **42**, 511–515.

Dyková I. & Novoa B. (2001) Comments on diagnosis of amoebic gill disease (AGD) in turbot, *Scophthalmus maximus*. *Bulletin of the European Association of Fish Pathologists* **21**, 40–44.

Dyková I., Figueras A. & Peric Z. (2000) *Neoparamoeba* Page, 1987: light and electron microscopic observations on six strains of different origin. *Diseases of Aquatic Organisms* **43**, 217–223.

Dyková I., Nowak B.F., Crosbie P.B., Fiala I., Peckova H., Adams M.B., Machackova B. & Dvorakova H. (2005) *Neoparamoeba branchiphila* n. sp., and related species of the genus *Neoparamoeba* Page, 1987: morphological and molecular characterization of selected strains. *Journal of Fish Diseases* **28**, 49–64.

Dyková I., Nowak B., Peckova H., Fiala I., Crosbie P. & Dvorakova H. (2007) Phylogeny of *Neoparamoeba* strains isolated from marine fish and invertebrates as inferred from SSU rDNA sequences. *Diseases of Aquatic Organisms* **74**, 57–65.

Dyková I., Fiala I. & Peckova H. (2008) *Neoparamoeba* spp. and their eukaryotic endosymbionts similar to *Perkinsela amoebae* (Hollande, 1980): coevolution demonstrated by SSU rRNA gene phylogenies. *European Journal of Protistology* **44**, 269–277.

Feehan C.J., Johnson-Mackinnon J., Scheibling R.E., Lauzon-Guay J.-S. & Simpson A.G.B. (2013) Validating the identity of *Paramoeba invadens*, the causative agent of recurrent mass mortality of sea urchins in Nova Scotia, Canada. *Diseases of Aquatic Organisms* **103**, 209–227.

Fringuelli E., Gordon A.W., Rodger H., Welsh M.D. & Graham D.A. (2012) Detection of *Neoparamoeba perurans* by duplex quantitative Taqman real-time PCR in formalin-fixed, paraffin-embedded Atlantic salmonid gill tissues. *Journal of Fish Diseases* **35**, 711–724.

Karlsbakk E., Olsen A.B., Einen A.C.B., Mo T.A., Fiksdal I.U., Aase H., Kalgraff C., Skar S.A. & Hansen H. (2013) Amoebic gill disease due to *Paramoeba perurans* in ballan wrasse (*Labrus bergylta*). *Aquaculture* **412–413**, 41–44.

Kent M.L., Sawyer T.K. & Hedrick R.P. (1988) *Paramoeba pemaquidensis* (Sarcomastigophora: Paramoebidae) Infestation of the gills of coho salmon *Oncorhynchus kisutch* reared in sea water. *Diseases of Aquatic Organisms* **5**, 163–169.

Kim H.J., Cho J.B., Lee M.K., Huh M.D. & Kim K.H. (2005) *Neoparamoeba* sp. Infection on Gills of Olive Flounder, *Paralichthys olivaceus* in Korea. *Journal of Fish Pathology* **18**, 125–131.

Lee L.E.J., Van Es S.J., Walch S.K., Rainnie D.J., Donay N., Summerfield R. & Cawthorn R.J. (2006) High yield and rapid growth of *Neoparamoeba pemaquidensis* in co-culture with a rainbow trout gill-derived cell line RTgill-W1. *Journal of Fish Diseases* **29**, 467–480.

Lovy J., Becker J.A., Speare D.J., Wadowska D.W., Wright G.M. & Powell M.D. (2007) Ultrastructural examination of the host cellular response in the Gills of Atlantic Salmon, *Salmo salar*, with Amoebic Gill Disease. *Veterinary Pathology* **44**, 663–671.

Lumsden J.S., Ferguson H.W., Ostland V.E. & Byrne P.J. (1994) The mucous coat on the gill lamellae of rainbow trout (*Oncorhynchus mykiss*). *Cell Tissue Research* **275**, 187–193.

Mitchell S.O. & Rodger H.D. (2011) A review of infectious gill disease in marine salmonid fish. *Journal of Fish Diseases* **34**, 411–432.

Morrison R.N., Crosbie P.B. & Nowak B.F. (2004) The induction of laboratory-based amoebic gill disease revisited. *Journal of Fish Diseases* **27**, 445–449.

Mouton A., Crosbie P., Cadoret K. & Nowak B. (2014) First record of amoebic gill disease caused by *Neoparamoeba perurans* in South Africa. *Journal of Fish Diseases* **37**, 407–409.

Munday B.L., Lange K., Foster C., Lester R.J.G. & Handlinger J. (1993) Amoebic gill disease of sea-caged salmonids in Tasmanian waters. *Tasmanian Fisheries Research* **28**, 14–19.

Nowak B.F., Carson J., Powell M.D. & Dyková I. (2002) Amoebic Gill Disease in the marine environment. *Bulletin of the European Association of Fish Pathologists* **22**, 144–147.

Page F.C. (1983) *Marine Gymnamoebae*. Institute of Terrestrial Ecology, Natural Environment Research Council, p. 13. The Lavenham Press, Great Britain

Powell M.D., Leef M.J., Roberts S.D. & Jonesk M.A. (2008) Neoparamoebic gill infections: host response and physiology in salmonids. *Journal of Fish Biology* **73**, 2161–2183.

Rodger H.D. & Mcardle J.F. (1996) An outbreak of amoebic gill disease in Ireland. *Veterinary Record* **139**, 348–349.

Roubal F.R., Lester R.G.J. & Foster C.K. (1989) Studies on cultured and gill-attached *Paramoeba* sp. (Gymnamoeba: Paramoebidae) and the cytopathology of paramoebic gill disease in Atlantic salmon, *Salmo salar* L. from Tasmania. *Journal of Fish Diseases* **12**, 481–492.

Santos M.J., Cavaleiro F., Campos P., Sousa A., Teixeira F. & Martins M. (2010) Impact of amoeba and scuticociliatidia infections on the aquaculture European sea bass (*Dicentrarchus labrax* L.) in Portugal. *Veterinary Parasitology* **171**, 15–21.

Serrano-Luna J., Pina-Vazquez C., Reyes-Lopez M., Ortiz-Estrada G. & De La Garza M. (2013) Proteases from *Entamoeba* spp. and pathogenic free-living amoebae as virulence factors. *Journal of Tropical Medicine*. **2013**, 890603. doi: 10.1155/2013/890603.

Speare D.J., Ferguson H.W., Beamish F.W.M., Yager J.A. & Yamashiro S. (1991a) Pathology of bacterial gill disease – sequential development of lesions during natural outbreaks of disease. *Journal of Fish Diseases* **14**, 21–32.

Speare D.J., Ferguson H.W., Beamish F.W.M., Yager J.A. & Yamashiro S. (1991b) Pathology of bacterial gill disease – ultrastructure of branchial lesions. *Journal of Fish Diseases* **14**, 1–20.

Steinum T., Kvellestad A., Ronneberg L.B., Nilsen H., Asheim A., Fjell K., Nygard S.M., Olsen A.B. & Dale O.B. (2008) First cases of amoebic gill disease (AGD) in Norwegian seawater farmed Atlantic salmon, *Salmo salar* L., and phylogeny of the causative amoeba using 18S cDNA sequences. *Journal of Fish Diseases* **31**, 205–214.

Taylor R.S., Muller W.J., Cook M.T., Kube P.D. & Elliott N.G. (2009) Gill observations in Atlantic salmon (*Salmo salar,* L.) during repeated amoebic gill disease (AGD) field exposure and survival challenge. *Aquaculture* **290**, 1–8.

Van Haastert P.J.M. (2011) Amoeboid cells use protrusions for walking, gliding and swimming. *PLoS One* **6**, e27532.

Villavedra M., To J., Lemke S., Birch D., Crosbie P., Adams M., Broady K., Nowak B., Raison R.L. & Wallach M. (2010) Characterisation of an immunodominant, high molecular weight glycoprotein on the surface of infectious *Neoparamoeba* spp., causative agent of amoebic gill disease (AGD) in Atlantic salmon. *Fish & Shellfish Immunology* **29**, 946–955.

Young N.D., Dyková I., Snekvik K., Nowak B.F. & Morrison R.N. (2008) *Neoparamoeba perurans* is a cosmopolitan aetiological agent of amoebic gill disease. *Diseases of Aquatic Organisms* **78**, 217–223.

Young N.D., Dyková I., Crosbie P.B., Wolf M., Morrison R.N., Bridle A.R. & Nowak B.F. (2014) Support for the coevolution of *Neoparamoeba* and their endosymbionts, *Perkinsela amoebae*-like organisms. *European Journal of Protistology* **50**, 509–523.

Zilberg D. & Munday B.L. (2000) Pathology of experimental amoebic gill disease in Atlantic salmon, *Salmo salar* L. and the effect of pre-maintenance of fish in sea water on the infection. *Journal of Fish Diseases* **23**, 401–407.

Received: 1 July 2015
Revision received: 4 November 2015
Accepted: 4 November 2015

